Mechanical and Aerospace Engineering
P. Daponte (Ed.)
© 2025 The Authors.
This article is published online with Open Access by IOS Press and distributed under the terms of the Creative Commons Attribution Non-Commercial License 4.0 (CC BY-NC 4.0).
doi:10.3233/ATDE250392

Collaborative Robotic Finishing Platform for Metal Part Processing Towards Industry 5.0

Seyedhossein Hajzargarbashi[a,1] , Gabriel Côté [a], Jonathan Boisvert [a], Ramy Meziane [a], Chen Xu [b], Corentin Hubert [c], Sabrina Jocelyn [d], and Clément Gosselin [b]
[a] *National Research Council Canada (NRC)*
[b] *Université Laval*
[c] *École Polytechnique de Montréal*
[d] Institut de recherche Robert-Sauvé en santé et en sécurité du travail (IRSST)
ORCiD ID: Seyedhossein Hajzargarbashi https://orcid.org/0009-0004-5494-7985

Abstract. Manual finishing operations in aerospace and ground transportation industries are often associated with health-and-safety-related issues such as musculoskeletal disorders, productivity loss, and challenges in workforce renewal. This work presents an innovative automated solution to address these challenges, prioritizing the ease of implementation and affordability for small and midsize enterprises (SMEs). Our proposed solution is a collaborative robotic (cobotic) finishing platform designed to eliminate labor-intensive work while keeping human operators in the loop to manage unforeseen situations. This platform aims to eliminate health risks, enhance repeatability, improve product quality, and increase productivity. This paper describes the mechanical design of the platform, its embedded cyber-physical system (CPS), interactivity features, as well as its risk assessment and risk mitigation. The platform integrates a UR10 cobot mounted upside down on a gantry structure to expand workspace, along with 3D sensors, scene cameras, compliance end-effectors, a dust collection system, programmable logic controllers (PLCs), and augmented reality projectors to assist the operator for easy execution of finishing tasks. The CPS comprises interconnected physical twins, their models, and relevant packages for the control of the whole finishing process from PLC to autonomous robot programming. Safety measures, including safety-rated devices, attenuation measures, and personal protective equipment, are integrated to ensure operator's safety. While many research streams are fully integrated into the platform and CPS, some are still in the process of integration. Despite this, various finishing tasks have been successfully executed using the platform, demonstrating its potential to transform metal part finishing processes in industry.

Keywords. Cobot, Finishing operations, Compliance, Cyber-Physical System, ROS, Toolpath generation, Autonomous path planning, Parallel robot, Risk assessment, Implicit surface representation, Meshing, Point cloud alignment, Pose refinement, Volumetric grid, Human-machine interaction, Gesture recognition

1. Introduction

The manufacturing sector, especially in aerospace and ground transportation verticals, has traditionally relied on manual labor for metal part finishing, including deburring, edge chamfering, shot peening, sanding, and polishing. These labor-intensive tasks pose

[1] Corresponding Author: Seyedhossein Hajzargarbashi, Aerospace Research Centre, National Research Council Canada (NRC), Montréal, Canada, Seyedhossein.Hajzargarbashi@nrc-cnrc.gc.ca .

health-and-safety-related risks, contribute to low productivity, and present workforce renewal challenges since they are less attractive. Automation of these operations could potentially eliminate associated health risks, improve repeatability and product quality, and increase productivity. However, this automation faces some challenges due to the inherent variability in workpiece geometries, tool characteristics, and the non-repetitive nature of these tasks [1]. The difficulty to anticipate all potential variations and preprogram a robot to handle them effectively has limited automated finishing to production lines with tightly controlled variations [2]. This paper attempts to provide solutions for these challenges and proposes a human-centric innovative solution towards the ideal concept conveyed by Industry 5.0 [3], which “complements the existing "Industry 4.0" approach by specifically putting research and innovation at the service of the transition to a sustainable, human-centric and resilient” industry [4]. The proposed cobotic finishing platform enables human operators to collaboratively supervise the finishing process, thus allowing more resilience when facing unforeseen situations.

A collaborative application is a process comprising at least one part of the industrial robot sequence where the robot, its robotic tool, the part being handled or worked on, the equipment or obstacles influencing the risks in use, and the operator are in the same protected space [5]. The University of Southern California has led researches to the formulation of algorithms for finishing tasks using a KUKA LBR iiwa robot, inherently designed for collaborative applications (cobot) [1], [6], [7]. These works were primarily focused on the automated generation of trajectories and part setups, which were successful in multiple application scenarios but could be time-consuming for complex geometries. Factors such as variations in geometry, the management of the as-built condition of the part, and interaction with humans received less attention.

On the other hand, there has been a growing corpus of research on human-robot collaboration. For instance, Peternel [8] used a cobot to position the part in front of the operator, thereby facilitating the operator's working conditions during polishing operations. A force control scheme was integrated into a cobot to replicate the force profile of manual finishing operations performed by an operator, using deep neural networks [9]. An industrial robot was used in a human-robot collaborative finishing task to replace operators in initial less demanding phases (simple geometries and looser tolerances) [10], [11], while operators finalized the finishing of more complex features. In these studies, the primary method for motion planning remained offline programming, which is not only time-consuming but also requires expensive licenses. The management of geometric variations relied on operators manually completing parts based on their experience.

In order to provide a robust solution, this collaborative research aims to develop innovative approaches for an interactive collaborative finishing platform. This would enable complete and robust automation of the finishing process for complex metallic parts with unstructured geometric features (e.g., irregular weld spatters). One objective is to eliminate the need for dedicated jigs and tools to conform the part geometry to its nominal state, allowing the system to handle the part geometry as it was built and as it is fixed to the table. Several interactive tools have been developed to assist operators in defining and modifying optimum finishing setups/tasks without requiring further manual operations or programming skills. Deep learning is utilized to enhance interactivity by recognizing the operator’s gestures via the vision system.

This paper proposes a solution that leverages 3D scanning data to create an accurate 3D model of the actual part, along with a method to reduce or eliminate offline robot programming. A user-friendly human-machine interface has been developed, enabling

operators to interactively assign tools and process parameters to selected surfaces/curves and modify them during task execution if necessary. The physical human-robot interaction is facilitated by using a cobot and the CPS with touchscreen and gesture recognition capabilities. A data-driven neural network will be integrated in future works, further assisting operators in selecting the best parameters for obtaining the desired quality.

This paper details the mechanical design and development of the platform in section II. The developed platform includes a cobot and auxiliary linear axis, sensors including a 3D scanning system for part digitization and scene cameras for gesture recognition, two integrated controllers, and a newly developed programmable tri-axial compliance head. Section III describes the CPS and integrated functionalities specific to the finishing operation. The CPS extends beyond an interconnected network of digital twins to include 3D model reconstruction, adaptive path planning, and robot motion and setup optimization. In section IV, the interactivity via touchscreen and gesture recognition is explained, while section V covers the risk assessment and risk mitigation of the platform.

2. Cobotic Platform Architecture

A collaborative robotic platform has been purposefully designed, as illustrated in Figure 1, to serve as a dedicated testbed for cobotic industrial applications within the Aerospace Manufacturing Technologies Centre (AMTC) at the National Research Council of Canada (NRC). An ergonomically designed downdraft table complements the setup, facilitating efficient part handling and clamping for the operator.

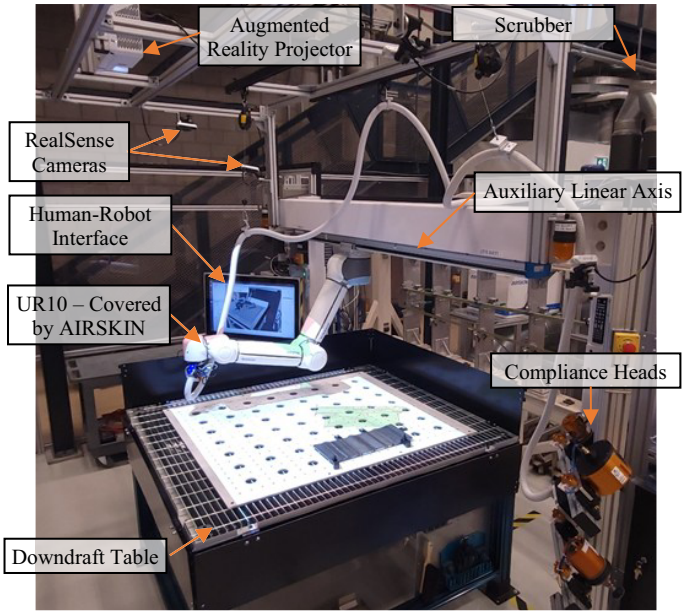

Figure 1. Cobotic Finishing platform developed at the NRC

2.1. Robot and Auxiliary Linear Axis

The platform includes a UR10/CB3 cobot mounted upside down on a linear range extender, which is supported by a fixed gantry structure. This configuration expands the robot workspace and reduces the number of setups required to finish parts measuring up to 1.2m x 1.2m horizontally.

2.2. Sensors

Extensive knowledge of the 3D geometry of the object requiring finishing operations is necessary to establish tool paths and make informed decisions about the state and quality of the current fabrication step. Furthermore, three-dimensional information about the human(s) present in the work cell is also needed in order to gather user feedback on the current tasks, to plan the next steps and also to ensure the safety while work is being performed.

The choice was therefore made to equip the cobotic platform with different kind of optical 3D sensors to collect information necessary for task planning and user interaction. Two types of sensors were selected: one that is attached to the end-effector of the cobotic manipulator to digitize the manipulated object with precision, while another type of sensor is responsible for monitoring the work cell. Performance requirements for the types of sensors are different. The end-effector sensor needs enough precision, resolution, and accuracy to guide the fabrication and evaluate potential defects. For this task, a structured-light sensor Gocator 3210 from LMI (Burnaby, Canada) was selected (Figure 2). The VDE/VDI [12] accuracy claimed for this particular sensor is 0.035mm [13], which was deemed appropriate for the application.

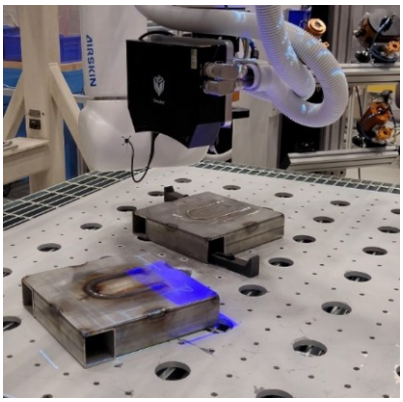

Figure 2. LMI Gocator 3210 integrated to the platform

In the case of work cell monitoring, the accuracy and resolution requirements are not as stringent. The goal is to be able to interpret human motion and act accordingly. However, volume coverage is a greater challenge. Multiple items (e.g. the robot arm itself, the table, the rail system, or even human users) can obstruct the sensor's line of sight. The solution in this case was to select cheaper 3D sensors and to install multiple units. In this context, the Intel RealSense D455 was selected [14] and six units were installed, two of which are visible in Figure 1.

Contrary to its newer version, the UR10e, which comes with a built-in Force/Torque (FT) sensor, the cobot used in the platform, the UR10, does not have an FT sensor. A Robotiq FT sensor has been added to the robot to enable force and torque readings during finishing operations.

2.3. Compliance Head

In order to ensure the quality of finished parts, it is crucial to control the finishing force exerted by the robot on the workpiece surface. Excessive force can lead to defects, damage, or inconsistencies in the final part, while insufficient force may result in an incomplete finish. Therefore, robust control of the normal finishing force in robotic applications is essential to optimize quality, reduce waste, and increase overall productivity. However, robots are limited by their control bandwidth, restricting their use to applications with low dynamics. It has been demonstrated that a robot with active force control struggles to apply the correct force in parts requiring fast orientation changes and/or high velocity, and it can encounter instability [15]. To overcome this challenge and ensure stable material removal, especially for complex surfaces, a common practice is to use compliance tool holders [16], referred to hereafter as compliance heads.

The developed platform is outfitted with three passive compliance heads: two axially compliant with idle speeds of 5600 rpm and 15000 rpm, and a radially compliant one with an idle speed of 30000 rpm. With these passive compliance heads, the desired force is adjusted by air pressure for a specific tool inclination at the start of the operation, without any closed-loop control. There are also active compliance heads that feature embedded closed-loop feedback control, which actively adjusts the compliance during the operation. According to our market study, all commercially available compliance heads have only one compliant direction, necessitating tool head changes between various operations.

In order to alleviate the drawbacks of existing compliance tools, namely the stability issues and the inability to control the stiffness in multiple directions, a novel compliance head is proposed in this paper. The compliance head consists of a backdrivable three degree-of-freedom (DoF) actuated translational parallel mechanism. The backdrivability of the system allows the use of an impedance control approach instead of the conventional admittance control approach, thereby leading to a very responsive and stable behaviour. Another advantage of the impedance control scheme is that it does not require the use of a force/torque sensor. Moreover, the stiffness of the device can be assigned independently in all three Cartesian directions instead of only in a direction normal to the contact surface. This allows the tool to follow contours while performing metal finishing tasks.

The architecture of the compliance head is first selected. Based on potential kinetostatic performances [17], the architecture of the delta robot is chosen [18]. This robot architecture allows the positioning of a platform in three-dimensional space while providing stiffness and agility. The architecture of the mini robot (compliance head) is shown in Figure 3(a).

In this architecture, the actuators are connected to the base joints of the delta mechanism through toothed belts, yielding a transmission ratio of 3:1. This ratio amplifies the motor torques while still providing easy backdrivability. The reduction

ratio was selected to optimize the transmission efficiency, namely to remain close to the ratio of inertia between the actuator and the moving links, i.e.,

$$\eta = \sqrt{(J_m/J_i)} \qquad (1)$$

where J_m is the inertia of the mechanism and J_i is the inertia of the actuator. Based on the mechanical characteristics of the robot, the above calculation yields a value of η of approximately 2.2, and hence a ratio of 3 is selected, which ensures that the robot design is very close to being optimal while ensuring a proper amplification of the motor torques. Given this arrangement, the geometry of the mechanism and the capabilities of the actuators, the compliance head can provide forces of approximately 150 N in the direction normal to the tool and of approximately 60 N in the other directions, which is deemed sufficient for many finishing operations. The prototype of the compliance head is shown in Figure 3(b).

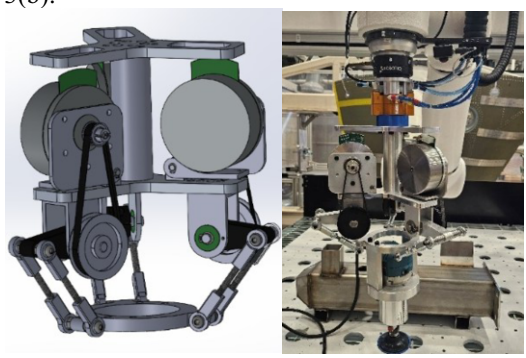

(a) (b)

Figure 3. (a) Architecture of the compliance head. The large cylinders at the top are the actuators while the annulus at the bottom is the end-effector. (b) Prototype of the compliance head integrated to the platform.

As mentioned above, the control of the robot is based on an impedance control scheme [19], to which a gravity compensation term is added. The orientation of the tool with respect to gravity is provided by the configuration of the robot on which the compliance head is mounted. The control law can then be written as

$$\tau = (J^{-1}K)^T\,(B\Delta\dot{x} + C\Delta x) + \tau_g \qquad (2)$$

where τ is the actuator torque, J and K are the forward and inverse Jacobian matrices of the parallel robot, B and C are the prescribed damping and stiffness matrices according to the impedance control law, Δx is the Cartesian displacement vector of the robot end-effector and τ_g is the gravitational torque.

Experimental validations have been conducted in which a force/torque sensor was used to measure the applied force and compare it to the prescribed force. Although the force/torque sensor is not used in the controller (it is only used to collect ground truth data), it can be observed that the commanded force is closely matched by the robot.

2.4. Controller

The Robot Operating System (ROS) is a flexible framework that facilitates communication between various components of a robotic system, such as robots, sensors, actuators, and other devices, through its extensive libraries. However, there are instances where certain devices may not be compatible with ROS. This could be due to the absence of ROS-compatible drivers, the requirement of specific protocols that ROS does not support, or the lack of modern communication interfaces in the devices. Additionally, ROS does not inherently support real-time operations, which can be a limitation for safety-critical devices or those with strict real-time requirements. To overcome these challenges, PLCs can be integrated into the cobotic platform. PLCs can provide the necessary real-time control with bidirectional and reliable communication and are compatible with a wider range of devices, thereby enhancing the functionality and safety of the system.

Soft PLCs, operating in accordance with the IEC 61131 standard much like their traditional hardware counterparts, have emerged as cost-effective and flexible solutions that can be implemented on any reliable computing platform. Among these, CODESYS has gained prominence in recent years as a benchmark Soft PLC. Its integration with ROS has been demonstrated in several applications [20]. However, for the development of our cobotic platform, we have chosen to utilize a well-established hardware PLC, specifically the Allen Bradley 1769-L30ER Compactlogix. This decision was made to keep our focus on the primary objective of delivering a collaborative finishing solution, rather than venturing into the exploration of a novel approach. Our CPS communicates with the PLC using libplctag [21], an open-source library, through EtherNet/IP to read and write tags in the PLC. This enables the management of various components such as compliance heads, the tool magazine, the tool changing system, the scrubber for dust collection and indicator lights. Additionally, the CPS communicates with a safety PLC, which is responsible for the safety circuit of the platform.

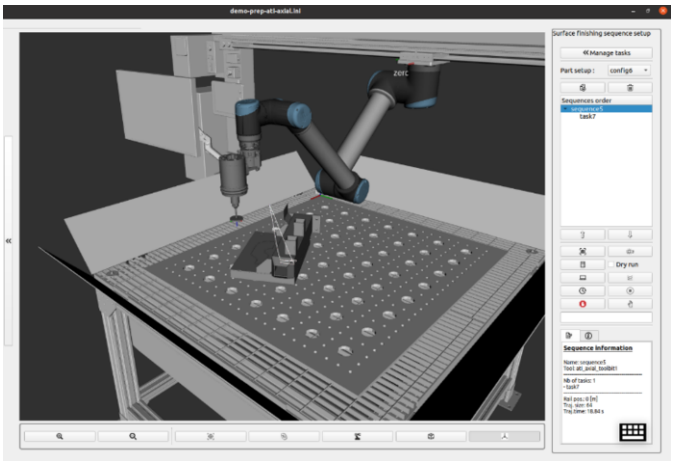

Figure 4. CPS GUI for finishing operations

3. Cyber-Physical System

The digital twins of the platform components, such as the cobot, linear extender, and tools, and their physical twins, are integrated and interconnected within a CPS. The CPS also includes a model layer and an application layer composed of various software components. At the core of this network is a compact industrial PC running on Linux, with multiple computational modules developed and interfaced through ROS. The application layer integrates main functionalities such as 3D model importing and geometry management, finishing task definition, toolpath generation, robot motion and setup optimization, and simulation. The CPS has several advantages, including synchronized digital/physical states of its components, flexibility to adapt to varying conditions of the part, decision-making tools for the operator, and improved system safety. To interact with the CPS, a user-friendly graphical user interface (GUI), depicted in Figure 4, serves as its front-end.

3.1. Standard ROS packages

ROS is an open-source framework designed for robotics applications, which comprises a collection of software libraries, algorithms and tools. Its modular design makes it a perfect match for the cyber-physical system presented in this paper, as it integrates components from diverse academic and research collaborators [22].

Aside from our own packages introduced by this paper in section III (B-D), the following standard ROS packages are used:

- *Moveit*, a robot motion planning framework, for the generation of collision-free trajectories from the robot's home position to approach position and retract position to home position [23].
- *Universal Robots ROS Driver,* which acts as an interface between ROS and the UR10 robot, facilitating the retrieval of robot states and the transmission of commands such as the execution of joint or cartesian trajectories [24].
- *RViz*, the 3D visualizer for ROS, to visualize the digital twin in real-time as seen in Figure 4. Implemented as a Qt widget, it is easily integrated in our own GUI as the central visualization widget [25].
- *InteractiveMarkers,* an add-on to RViz*,* which allows the user to interact with RViz markers, enabling, as an example, the selection of specific geometric features on the workpiece to program finishing tasks and generate toolpaths [26].

3.2. 3D Model Reconstruction

To be able to perform finishing operations, it is essential to be able to compare the actual geometry of the part with its CAD model and to quantify the differences between the two. It may also be relevant to build a triangulated model (mesh) of the part for visualization purposes since a mesh is more suited to efficient visualization and graphics rendering than a raw point cloud.

With regard to the former task, we used an implicit surface modeling approach based on the vector field implicit surface representation [27]. A volumetric grid made up of voxels of a given size is used to construct the triangulation. The scan data is read and the

covariance matrix of the 3D points falling into each voxel is calculated. The surface normal n is the smallest eigenvalue of this matrix. For each voxel, it is assumed that the surface it contains is flat of normal n. This planarity hypothesis is valid if the size of the voxels is small enough. Once the vector field is completed, the triangulation is constructed by applying the Marching Cubes algorithm [28] to the implicit representation contained in it. Figure 5(a) and (b) show two triangulations obtained from a scan for two sizes of voxels. An advantage of this approach is that the triangles in the mesh are almost equiangular, a situation that is rarely met for meshes built directly from the point cloud.

As for the comparison between the scan and the CAD model of the part, this step has been divided into two phases. The first phase, which is performed off-line, consists of associating points of a scan of a reference part to the same points on the CAD model. The reference part is considered as one without deformation that has been built in good conformity with its model. Figure 5(c) and (d) show the CAD model and the scan of the part with four matching points. With these matches, a rigid transformation between the reference frame of the part (which is installed in a controlled position on the cyber-physical bench) and the reference frame of the CAD model is estimated with Umeyama's implementation of the Kabsch's method [29]. The second phase, which is on-line and fully automatic for all parts other than the reference part, is comprised of three steps. The first step is to downsample the point cloud of the scan of the part to be inspected and eliminate the outliers. The normal at the surface of each point of the undersampled cloud is estimated. Planar geometric primitives are detected by a region growing algorithm using the normals. The points belonging to the plane primitives are transformed in the CAD model frame with the transformation obtained in phase 1. Points belonging to non-deformed plane primitives (i.e. points that are at a short distance from the CAD model) are retained and are used for the second step, which consists of refining the scan alignment with respect to the CAD model with an ICP-based approach [30]. The third step is to estimate the shortest distance between each point of the scan aligned with the CAD model to characterize the deformation of the part with its model.

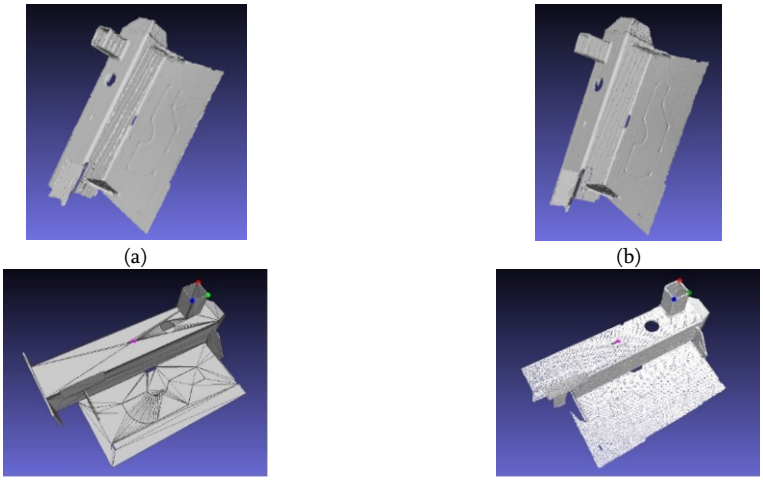

(a) (b) (c) (d)

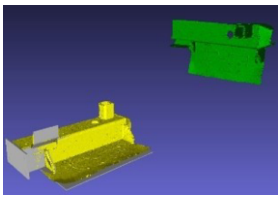

(e)

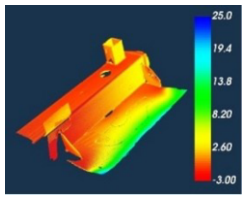

(f)

Figure 5. (a) Mesh model with 2 mm resolution of vector field. (b) Mesh model with 1 mm resolution of vector field. (c) CAD model with selected alignment points (d) Scan with selected aligment points. (e) Final alignment of the scan (yellow) on the CAD model (grey). (f) Heat map of distance between scan and CAD model.

3.3. Adaptive Toolpath Generation

A toolpath is the starting point for generating robot programs for finishing applications. The selected geometry must be discretized into linear segments of appropriate lengths to ensure accurate robot motions and effective collision prevention. A linear segment is more suitable compared to arc segments due to its simplicity of calculations and control concerns. Geometry segmentation has commonly been used to describe the geometric features [31] using a UV grid [32] or adaptive spacing between finishing curves [33]. In most of these approaches, the finishing curve segmentation is performed at equal distances without adapting to the surface geometry. Unlike traditional Computer-Aided Manufacturing (CAM) software applications, Rhino Grasshopper (RG) allows the integration of plug-ins [34], [35] for custom toolpath generation. However, RG employs interconnecting modules for toolpath generation that may decrease its user-friendliness for operators in the industrial field. Furthermore, the use of commercial CAM software for developing robotic solutions for SMEs is often not ideal due to its high cost, complexity, and limited customization capabilities. The Bezier package [36] is an open-source toolpath generation module compatible with ROS, but it is not an adaptive approach. The user needs to decrease the distance between generated poses to approximate the curved geometry, which results in high number of poses even for the linear portion of the geometry. For efficient toolpath generation, the number of toolpath poses must be adapted based on the geometry curvature. This consequently enhances the robot controller behavior and avoids control saturation.

A new approach has been developed to meet this adaptability requirement. This approach incorporates an adaptive toolpath generation algorithm where toolpath poses are determined based on the chosen geometry [37]. Depending on the geometric features, more toolpath points are created in the nonlinear parts and fewer in the linear parts. The algorithm enables effective adaptation to various geometric forms while resulting in a minimum number of generated toolpath poses. Moreover, the approach includes a collision control surface method to avoid collisions between the robot's end-effector (tools) and the selected surfaces of the workpiece. The toolpath poses that cause collision are identified and removed from the toolpath. The algorithm uses three parameters: toolpath tolerance, which defines the maximum permissible distance between a linear segment and the actual geometry; maximum distance between consecutive points, and safety offset to avoid collisions with respect to a surface. An intuitive dialog box has been added to the GUI to define the necessary elements and parameters for the algorithm and visualize the generated toolpath. Once the toolpath is generated, the robot's trajectory is produced as described in section III-D. This algorithm not only improves the accuracy

of toolpath generation, but also increases the robustness and flexibility of the robotic programming process.

3.4. Robot Motion and Setup Planning

After generating a toolpath in the local part reference frame, the next step is to plan the setup and the robot motion. The cobotic platform (see Figure 1) consists of a robot mounted on a rail (i.e. 7 DoF) and also allows positioning/orienting the part on the table thus providing an additional 3 DoF. Therefore, this particular operational framework offers an opportunity to exploit 5 optimization parameters to maximize process efficiency. These are the three coordinates (x,y,theta) defining the positioning of the part on the table (see Figure 6) as well as the rail coordinate and the rotational coordinate about the tool axis.

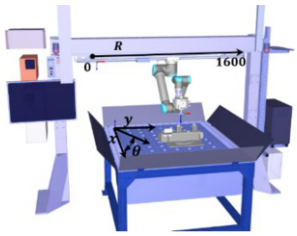

Figure 6. Representation of the cobotic workcell. The position and orientation $\boldsymbol{\theta}$ of the part on the table is expressed in frame ***[x,y]***. The linear axis position is expressed from 0 to 1600 *[mm]*.

Amongst the approaches that have been proposed in the art for robot motion and setup planning, Aspragathos [38] used a genetic algorithm (GA) to position the workpiece based on the higher mean value of a 'manipulability' index [39] along the path. Ur-Rehman et al. [40] focused on optimizing the motion of a 3 DoF parallel robot along a predefined path aiming to minimize the energy consumption, maximum applied torques to joints and shaking forces using a multi-objective GA. Lopes and Pires [41] employed a GA to reduce power consumption and enhance the Cartesian stiffness of a 6 DoF parallel robot. Malhan [7] introduced a workpiece positioning method with fast convergence to find feasible solutions under constraints such as joint limits, minimum velocity and force, collision and singularity. Ye et al. [42] optimized the workpiece setup on the table using particle swarm optimization (PSO) to minimize the contour error-based machining performance index (CEMPI) in milling operations. The CEMPI is defined based on the statistical properties of contour errors attributed to the robot's low stiffness.

Our literature review revealed a lack of comprehensive optimization solutions that simultaneously consider the entire environmental collision scene, workpiece placement, and efficient management of all external and/or redundant axes to generate collision-free robot trajectories. Moreover, none of the proposed solutions accommodated user-defined optimization conditions, such as manipulability, while also ensuring low computation time. Consequently, a novel approach is developed in this work to accommodate this larger set of requirements. An optimization problem is formulated, characterized by a non-linear, large, and complex solution space, along with various constraints such as collision and joint limits. The optimization problem involves simultaneously finding solutions for robot redundancy, the position of external axes, as well as for the position

and orientation of the workpiece position on the table (see 0). The objective function combines the robot condition number and the distance from the home position to the defined task in the joint space. While the condition number ensures that the robot stays away from singularities, the distance from the home position aids in reducing cycle time and preventing twisting of cables and hoses.

The proposed approach allows to find near optimal scenarios, with a high success rate, in minutes (thus quasi-real-time), making it compatible with industrialization.

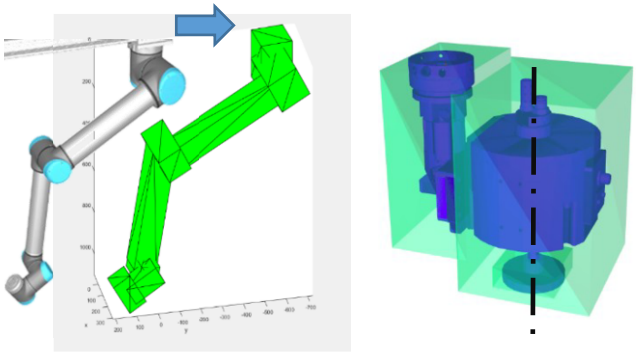

(a) (b)

Figure 7. The UR10 robot's geometry is approximated with cuboids (a) and the end-effector is approximated with bounding boxes (b).

This performance is achieved by:

1. Decomposing all workcell geometries into convex elements (such as the robot and end-effector shown in Figure 7) for collision detection, utilizing the Gilbert–Johnson–Keerthi (GJK) algorithm [43].
2. Implementing a GA optimization that includes the collision detection as a constraint.

4. Interactivity

Touchscreens have become ubiquitous in everyday life, with people getting used to interacting with various applications on their cell phones, tablets, and computers. Therefore, the touchscreen is selected as the primary interface between the operator and the CPS in this study. Touch gestures are intuitively defined to facilitate operator tasks such as the manipulation of 3D models, selection of geometric features, task definition, simulation-based verification, and execution of finishing operations. However, this solution requires the operator to move next to the screen whenever a command is necessary.

To enhance the operator's experience, human-robot interaction is best imagined through the interpretation of static hand gesture commands acquired by RGB-D cameras in the vicinity of the platform. A dictionary of 10 static hand gestures can be defined to start and end the communication, to run, cancel and repeat a command, and to encode a choice of tool, and its parameters.

Previous work on human-computer interface (HCI) has addressed hand gesture recognition [44], notably for collaborative workstations [45], and associated datasets are available to train models for the task [46]. However, in most cases, the operator is facing the camera. To offer flexibility to the operator, our goal is to automatically recognize the gesture regardless of the operator's position in the platform and regardless of the robot position (generating severe visual occlusions). Thus, six RGB-D sensors (Section B) are placed around the platform in a way to cover all the area accessible to the human operator around the table and to ensure that the operator can be always seen by at least two cameras.

For hand gesture recognition, a pipeline composed of three main steps is proposed:

1. Automatic hand detection in all images using a fine-tuned YOLO v8 model [47].
2. Automatic hand gesture classification using a ResNet model [48] trained from scratch, given the detected hand regions from the previous step.
3. Multi-view aggregation by averaging the classification probabilities of the synchronous RGB-D image set.

To train and test our two models, a new dataset (called MVH for Multi-View Hand gesture) was collected in a way to account for variabilities in visual occlusions, human subjects, positioning, and lighting conditions [49]. It comprises more than 85,000 RGB-D images of 20 participants, recorded through six different points of view, performing 10 gestures each with either hand, at various locations in the platform. The robot was moved several times during data collection to create variable occlusions. This unique dataset with its annotations will soon be made available to the community.

Tab. I provides the quantitative results of a 5-fold cross validation of the hand detection and gesture classification models, trained and tested on MVH and on the public dataset (HANDS) used in [46] for comparison. It shows first that the models trained on MVH provide a better generalization to the other dataset, rather than the other way around. This is attributable to the large variability offered by MVH. Second, the result of 93.7% accuracy in classification on HANDS demonstrates that our recognition model outperforms the state of the art on this dataset (90% [45]).

Table 1. Performance of hand detection (map) and gesture recognition (accuracy)

Trained on	**Tested on**			
	HANDS		**MVH**	
	mAP	**Accuracy**	**mAP**	**Accuracy**
HANDS	0.993	93.7%	0.063	35.1%
MVH	0.847	96.6%	0.955	86.0%

Finally, the aggregation of multiple synchronized views (step 3) increases the accuracy of the hand gesture recognition pipeline by 11% and improves the robustness to visual occlusions inherent to the cobotic context.

The performance obtained with the proposed hand gesture recognition pipeline using a vision-based communication channel motivates our ongoing efforts to integrate this solution in ROS to carry out the communication with the robot.

5. Safety

While the cobot performs a finishing task, the human operator supervises the process, controls the quality of the parts, and uses a gesture recognition system to indicate whether finishing tasks need to start, end, or be modified. In terms of occupational health and safety (OHS), a risk assessment was conducted during various phases of the platform's development. This approach is holistic in considering the cobot, humans, the surrounding environment and auxiliary equipment. Each hazardous situation was identified by associating risk indexes, which are based on the combination of the severity of the harm and its qualitative probability as per [50], and the draft of the next ISO 10218-2 [5].

The risk assessment of the platform identified 55 risks, each representing a distinct hazardous situation. These were assessed across six categories. A considerable number of these risks, notably all those within the electrical and noise categories, were determined to be at an acceptable level, thus necessitating no further mitigation measures. To shield operators near the platform from thermal risks, such as sparks and hot surfaces, it is mandatory for them to wear safety glasses, a visor, a lab coat, and gloves. Within the pneumatic risk category, the installation of an emergency cut-off valve on the main pneumatic line, along with the secure attachment and covering of hoses, contributes to risk reduction.

To address the chemical risk category, a dust collection system has been designed and approved for safe dust collection according to NFPA-484 [51]. It comprises a downdraft table and a 5000 SCFM scrubber. The platform is dedicated to processing only one material, whether aluminium or stainless steel, at a time. Any change in the material necessitates complete decontamination to mitigate explosion risks.

The mechanical risk category encompasses the most of high risks. The integration of the sensitive skin AIRSKIN onto the cobot [52] and the addition of emergency stop buttons (E-stop), have effectively reduced the cobot's motion-related risks to an acceptable level. This is further aided by the inherent reduced finishing advanced speed. The risk of compliance head ejection is mitigated by the tool changer's locking system and the mandatory use of safety shoes. The risk of workpiece ejection during the process is minimized by an appropriate clamping system, which includes a threaded tabletop and clamps.

The only remaining high risk is the potential contact between the rotating disc and the operator. Based on a survey conducted on industrial partners' premises, anti-cut gloves were initially considered as a measure to reduce this risk. However, extensive tests involving various grades of anti-cut gloves and grinding discs have shown their inefficiency. Consequently, two laser scanners have been integrated to detect the operator's presence and stop disc rotation when the operator approaches too closely. While this solution is accepted within a research environment, its applicability in industry needs validation. Ongoing efforts are focused on identifying a more reliable solution for industry, with the aim of enhancing the collaborative aspects of the proposed cobotic solution.

6. Discussion and Conclusion

This paper presents some enabling solutions for the challenges associated with automating manual labor-intensive finishing tasks. The proposed human-centric cobotic finishing platform represents an affordable and intelligent machine towards Industry 5.0,

offering productivity improvement, enhancing finishing quality, and mitigating health and safety risks. The platform is built of a UR10 cobot, various sensors, commercial and newly developed compliance heads. It provides a robust tool to operators within an innovative approach to define, evaluate, and modify finishing tasks of complex geometries. The integration of a CPS further enhances the platform's capabilities with a network of interconnected digital twins, data-driven interactivity, and improved system safety. Extensive experiments have validated the effectiveness of the developed technologies and allow debugging and fine-tuning of the platform and the CPS. Recently, 240 successful finishing tasks were conducted based on a design of experiments, taking into account various feed rates, compliance forces, tool angles, tool offsets, grit grades, and setup zones, to generate a rich dataset for ongoing machine learning research. This dataset provides a potential to predict surface roughness and to optimize process parameters, further enhancing the platform's capabilities. The ongoing exploration of machine learning applications represents a future direction for this research.

Acknowledgment

The authors wish to thank Bruno Monsarrat, Julien-Mathieu Audet, Pierre-Luc Beaulieu, Thierry Laliberté, Nathan Odic, Denis Laurendeau and Lama Seoud for their significant contributions to this paper. Unfortunately, due to limitations on the number of authors, their names could not be included. The authors also appreciate the NRC technical team, including Christian Corbeil, François Ferland, Henri Elame, Diego Garcia, Alexandre Gariépy, Guy Godin, David Liu and Michel Picard at the Aerospace Manufacturing Technologies Centre, Automotive and Surface Transportation Centre and Digital Technologies Research Centre. Their contributions to the construction of the cobotic platform enabled us to demonstrate the developed technologies. We are also thankful to the IRSST team, especially Damien Burlet-Vienney and Chantal Gauvin, for their contributions and insights in assessing and reducing the inherent risks associated with the platform. We also thank Michaël Lessard-Poulin, product expert at Prevost, and Gabriel Caron-Guillemette, project engineer at Alstom, both members of the project steering committee, for providing valuable insights and technical support.

The research studies reported in this paper are supported by the NRC's METALTec industrial research group, National Program Office, and the Metal Transformation Research and Innovation Consortium (CRITM).

References

[1] A. M. Kabir et al., "Robotic Finishing of Interior Regions of Geometrically Complex Parts," in Volume 3: Manufacturing Equipment and Systems, College Station, Texas, USA: American Society of Mechanical Engineers, Jun. 2018, p. V003T02A005.

[2] G. Côté, M. Meshreki, S. Zhongde, M. De Montigny, and S. Louvel, "Challenges in Robotized Polishing of Aerospace Components," presented at the CASI AERO, Toronto, Canada, May 2017.

[3] S. Nahavandi, "Industry 5.0—A Human-Centric Solution," Sustainability, vol. 11, no. 16, Art. no. 16, Jan. 2019,

[4] "Industry 5.0 - European Commission." Accessed: Mar. 30, 2024. [Online]. Available: https://research-and-innovation.ec.europa.eu/research-area/industrial-research-and-innovation/industry-50_en

[5] International Organization for Standardization, "Robotics — Safety requirements — Part 2: Industrial robot applications and robot cells (ISO/FDIS 10218-2)." International Organization for Standardization, Under development 2023.
[6] A. M. Kabir, B. C. Shah, and S. K. Gupta, "Trajectory Planning for Manipulators Operating in Confined Workspaces," in 2018 IEEE 14th International Conference on Automation Science and Engineering (CASE), Munich, Germany: IEEE, Aug. 2018, pp. 84–91.
[7] R. K. Malhan, A. M. Kabir, B. Shah, and S. K. Gupta, "Identifying Feasible Workpiece Placement with Respect to Redundant Manipulator for Complex Manufacturing Tasks," in 2019 International Conference on Robotics and Automation (ICRA), Montreal, QC, Canada: IEEE, May 2019, pp. 5585–5591.
[8] L. Peternel, C. Fang, N. Tsagarakis, and A. Ajoudani, "A selective muscle fatigue management approach to ergonomic human-robot co-manipulation," Robotics and Computer-Integrated Manufacturing, vol. 58, pp. 69–79, Aug. 2019,
[9] S. Hamdan, E. Oztop, and B. Ugurlu, "Force Reference Extraction via Human Interaction for a Robotic Polishing Task: Force-Induced Motion," in 2019 IEEE International Conference on Systems, Man and Cybernetics (SMC), Oct. 2019, pp. 4019–4024.
[10] E. Magrini, F. Ferraguti, A. J. Ronga, F. Pini, A. De Luca, and F. Leali, "Human-robot coexistence and interaction in open industrial cells," Robotics and Computer-Integrated Manufacturing, vol. 61, p. 101846, Feb. 2020,
[11] F. Pini and F. Leali, "Human-robot collaborative reconfigurable platform for surface finishing processes," Procedia Manufacturing, vol. 38, pp. 76–83, 2019,
[12] VDI/VDE-Gesellschaft Mess-und Automatisierungstechnik Standard, "VDI/VDE 2634 Blatt 2 - Optical 3-D measuring systems - Optical systems based on area scanning." Engl. VDI/VDE-Gesellschaft Mess- und Automatisierungstechnik, Aug. 2012. [Online]. Available: https://www.vdi.de/en/home/vdi-standards/details/vdivde-2634-blatt-2-optical-3-d-measuring-systems-optical-systems-based-on-area-scanning
[13] "Large Field of View 3D Snapshot Sensor | Gocator 3210 3D Smart Sensors | LMI Technologies." Accessed: Mar. 24, 2024. [Online]. Available: https://lmi3d.com/series/gocator-3210/
[14] M. Servi et al., "Metrological Characterization and Comparison of D415, D455, L515 RealSense Devices in the Close Range," Sensors, vol. 21, no. 22, Art. no. 22, Jan. 2021,
[15] S. Gadringer, H. Gattringer, and A. Mueller, "Assessment of force control for surface finishing – an experimental comparison between Universal Robots UR10e and FerRobotics active contact flange," Mechanical Sciences, vol. 13, no. 1, pp. 361–370, Apr. 2022,
[16] W.-L. Zhu and A. Beaucamp, "Compliant grinding and polishing: A review," International Journal of Machine Tools and Manufacture, vol. 158, p. 103634, Nov. 2020,
[17] G. Jeanneau, V. Bégoc, and S. Briot, "Geometrico-Static Analysis of a New Collaborative Parallel Robot for Safe Physical Interaction," presented at the ASME 2020 International Design Engineering Technical Conferences and Computers and Information in Engineering Conference, American Society of Mechanical Engineers Digital Collection, Nov. 2020.
[18] F. Pierrot, C. Reynaud, and A. Fournier, "DELTA: a simple and efficient parallel robot," Robotica, vol. 8, no. 2, pp. 105–109, Apr. 1990,
[19] R. J. Anderson and M. W. Spong, "Hybrid impedance control of robotic manipulators," IEEE Journal on Robotics and Automation, vol. 4, no. 5, pp. 549–556, Oct. 1988,
[20] R. Arrais, P. Ribeiro, H. Domingos, and G. Veiga, "ROBIN: An open-source middleware for plug'n'produce of Cyber-Physical Systems," International Journal of Advanced Robotic Systems, vol. 17, no. 3, 2020,
[21] "libplctag," libplctag - a library for PLC communication. Accessed: Mar. 18, 2024. [Online]. Available: https://libplctag.github.io/
[22] "ROS: Home." Accessed: Mar. 24, 2024. [Online]. Available: https://www.ros.org/
[23] "MoveIt Motion Planning Framework." Accessed: Mar. 24, 2024. [Online]. Available: https://moveit.ros.org/
[24] "UniversalRobots/Universal_Robots_ROS_Driver." Universal Robots A/S, Mar. 20, 2024. Accessed: Mar. 24, 2024. [Online]. Available: https://github.com/UniversalRobots/Universal_Robots_ROS_Driver
[25] "ros-visualization/rviz." ros-visualization, Mar. 22, 2024. Accessed: Mar. 24, 2024. [Online]. Available: https://github.com/ros-visualization/rviz
[26] "ros-visualization/interactive_markers." ros-visualization, Feb. 23, 2024. Accessed: Mar. 24, 2024. [Online]. Available: https://github.com/ros-visualization/interactive_markers
[27] D. Tubic, P. Hebert, J.-D. Deschenes, and D. Laurendeau, "A unified representation for interactive 3D modeling," in Proceedings. 2nd International Symposium on 3D Data Processing, Visualization and Transmission, 2004. 3DPVT 2004., Sep. 2004, pp. 175–182.
[28] W. E. Lorensen and H. E. Cline, "Marching cubes: A high resolution 3D surface construction algorithm," SIGGRAPH Comput. Graph., vol. 21, no. 4, pp. 163–169, Aug. 1987,

[29] S. Umeyama, "Least-squares estimation of transformation parameters between two point patterns," IEEE Transactions on Pattern Analysis and Machine Intelligence, vol. 13, no. 4, pp. 376–380, Apr. 1991,
[30] A. W. Fitzgibbon, "Robust registration of 2D and 3D point sets," Image and Vision Computing, vol. 21, no. 13, pp. 1145–1153, Dec. 2003,
[31] J. Liu, X. Huang, S. Fang, H. Chen, and N. Xi, "Industrial robot path planning for polishing applications," in 2016 IEEE International Conference on Robotics and Biomimetics (ROBIO), Dec. 2016, pp. 1764–1769.
[32] S. McGovern and J. Xiao, "UV Grid Generation on 3D Freeform Surfaces for Constrained Robotic Coverage Path Planning," in 2022 IEEE 18th International Conference on Automation Science and Engineering (CASE), Aug. 2022, pp. 1503–1509.
[33] S. Schneyer, A. Sachtler, T. Eiband, and K. Nottensteiner, "Segmentation and Coverage Planning of Freeform Geometries for Robotic Surface Finishing," IEEE Robotics and Automation Letters, vol. 8, no. 8, pp. 5267–5274, Aug. 2023,
[34] J. Braumann and S. Brell-Cokcan, "Parametric Robot Control: Integrated CAD/CAM for Architectural Design," pp. 242–251, 2011,
[35] M. Adamik, A. Babinec, and L. Chovanec, "Tool Path Generator for Artistic Drawing with Industrial Robot," 2019 IEEE International Symposium on Measurement and Control in Robotics (ISMCR), pp. C2-3-1-C2-3–4, Sep. 2019,
[36] "ros-industrial-consortium/bezier." ROS-Industrial Consortium, Jan. 12, 2024. Accessed: Mar. 24, 2024. [Online]. Available: https://github.com/ros-industrial-consortium/bezier
[37] R. Meziane, J.-M. Audet, and S. H. H. Zargarbashi, "Adaptive Toolpath Generation for Wire Geometric Elements in Cyber-physical System for cobotic finishing," in 2024 IEEE 20th International Conference on Automation Science and Engineering (CASE), Aug. 2024, p. unpublished.
[38] N. A. Aspragathos, "Optimal Location of Path Following Tasks in the Workspace of a Manipulator Using Genetic Algorithms," in Recent Advances in Robot Kinematics, J. Lenarčič and V. Parenti-Castelli, Eds., Dordrecht: Springer Netherlands, 1996, pp. 179–188.
[39] T. Yoshikawa, "Manipulability of Robotic Mechanisms," The International Journal of Robotics Research, vol. 4, no. 2, pp. 3–9, Jun. 1985,
[40] R. Ur-Rehman, S. Caro, D. Chablat, and P. Wenger, "Multi-objective path placement optimization of parallel kinematics machines based on energy consumption, shaking forces and maximum actuator torques: Application to the Orthoglide," Mechanism and Machine Theory, vol. 45, no. 8, pp. 1125–1141, Aug. 2010,
[41] A. M. Lopes and E. J. S. Pires, "Optimization of the Workpiece Location in a Machining Robotic Cell," International Journal of Advanced Robotic Systems, vol. 8, no. 6, p. 73, Dec. 2011,
[42] C. Ye, J. Yang, H. Zhao, and H. Ding, "Task-dependent workpiece placement optimization for minimizing contour errors induced by the low posture-dependent stiffness of robotic milling," International Journal of Mechanical Sciences, vol. 205, p. 106601, Sep. 2021,
[43] M. Montanari and N. Petrinic, "OpenGJK for C, C# and Matlab: Reliable solutions to distance queries between convex bodies in three-dimensional space," SoftwareX, vol. 7, pp. 352–355, Jan. 2018,
[44] P. K. Pisharady and M. Saerbeck, "Recent methods and databases in vision-based hand gesture recognition: A review," Computer Vision and Image Understanding, vol. 141, pp. 152–165, Dec. 2015,
[45] C. Nuzzi et al., "MEGURU: a gesture-based robot program builder for Meta-Collaborative workstations," Robotics and Computer-Integrated Manufacturing, vol. 68, p. 102085, Apr. 2021,
[46] C. Nuzzi, S. Pasinetti, R. Pagani, G. Coffetti, and G. Sansoni, "HANDS: an RGB-D dataset of static hand-gestures for human-robot interaction," Data in Brief, vol. 35, p. 106791, Apr. 2021,
[47] D. Reis, J. Kupec, J. Hong, and A. Daoudi, "Real-Time Flying Object Detection with YOLOv8." arXiv, May 17, 2023.
[48] K. He, X. Zhang, S. Ren, and J. Sun, "Identity Mappings in Deep Residual Networks," in Computer Vision – ECCV 2016, B. Leibe, J. Matas, N. Sebe, and M. Welling, Eds., Cham: Springer International Publishing, 2016, pp. 630–645.
[49] C. Hubert, N. Odic, S. H. H. Zargarbashi, and L. Seoud, "MVH: multi-view hand gesture dataset for robust hand detection and gesture recognition in interactive robotic platform," Machine Vision and Applications, unpublished.
[50] International Organization for Standardization, "Safety of machinery — General principles for design — Risk assessment and risk reduction (ISO 12100:2010)." International Organization for Standardization, 2010.
[51] National Fire Protection Association, "NFPA 484 Standard for Combustible Metals." National Fire Protection Association, 2018.
[52] P. Svarny et al., "Effect of active and passive protective soft skins on collision forces in human–robot collaboration," Robotics and Computer-Integrated Manufacturing, vol. 78, p. 102363, Dec. 2022.